Crystal Structure of the FK506 Binding Domain of *Plasmodium falciparum* FKBP35 in Complex with FK506[†,‡]

Masayo Kotaka,[§] Hong Ye,[§] Reema Alag,[§] Guangan Hu,[§] Zbynek Bozdech,[§] Peter Rainer Preiser,[§] Ho Sup Yoon,*[,§] and Julien Lescar*[,§,||]

School of Biological Sciences, Nanyang Technological University, 60 Nanyang Drive, Singapore 637551, and AFMB, CNRS UMR6098, Marseille 13288, France

Received January 2, 2008; Revised Manuscript Received April 2, 2008

ABSTRACT: The emergence of multi-drug-resistant strains of *Plasmodium* parasites has prompted the search for alternative therapeutic strategies for combating malaria. One possible strategy is to exploit existing drugs as lead compounds. FK506 is currently used in the clinic for preventing transplant rejection. It binds to a α/β protein module of approximately 120 amino acids known as the FK506 binding domain (FKBD), which is found in various organisms, including human, yeast, and *Plasmodium falciparum* (PfFKBD). Antiparasitic effects of FK506 and its analogues devoid of immunosuppressive activities have been demonstrated. We report here the crystallographic structure at 2.35 Å resolution of PfFKBD complexed with FK506. Compared to the human FKBP12−FK506 complex reported earlier, the structure reveals structural differences in the $\beta5-\beta6$ segment that lines the FK506 binding site. The presence in PfFKBD of Cys-106 and Ser-109 (substituting for His-87 and Ile-90, respectively, in human FKBP12), which are 4−5 Å from the nearest atom of the FK506 compound, suggests possible routes for the rational design of analogues of FK506 with specific antiparasitic activity. Upon ligand binding, several conformational changes occur in PfFKBD, including aromatic residues that shape the FK506 binding pocket as shown by NMR studies. A microarray analysis suggests that FK506 and cyclosporine A (CsA) might inhibit parasite development by interfering with the same signaling pathways.

Malaria is a devastating disease affecting humans, with several hundred million cases worldwide and more than a million deaths per year (*1*). Human malaria is caused by infection with one of the four related intracellular protozoan species, *Plasmodium falciparum*, *Plasmodium vivax*, *Plasmodium ovale*, and *Plasmodium malariae*, which are transmitted by the female *Anopheles gambiae* mosquito vector. Among these, the *P. falciparum* parasite, which causes the most severe form of the disease, has developed resistance to many drugs currently in use (*2*), thereby prompting the search for new therapeutics. One possible strategy for the development of antiparasitic molecules is to exploit existing drugs or druglike compounds that are amenable to chemical modifications to render them more effective and specific against the parasite (*3*). FK506 is a 23-member macrolide lactone and potent immunosuppressant that binds to the peptidylprolyl cis−trans isomerase (PPIase)[1] domain (hence also known as the FK506 binding domain or FKBD) present in various FK506-binding proteins (FKBPs) (*4*). FKBPs constitute a large family of conserved proteins found across many organisms that assist protein folding by catalyzing the conversion of cis and trans rotamers of the peptidyl−prolyl amide bond of protein substrates (*5*). Although binding of FK506 to the FKBPs results in the inhibition of their PPIase enzymatic activity, its immunosuppressive activity has been demonstrated to occur for the human FKBP12 protein through an indirect mechanism that implicates calcineurin, a Ca^{2+}/calmodulin-dependent serine-threonine protein phosphatase. Once formed, the FK506−FKBP12 binary complex binds to calcineurin and inhibits its enzymatic activity. As a result, the level of phosphorylation of the NF-AT transcription factor decreases, impairing its translocation from the cytoplasm to the nucleus and leading to a temporary suppression of T- and B-cell functions (*6, 7*). Thus, FK506 and a new generation of its synthetic analogues are routinely prescribed to transplant recipients to prevent tissue rejection. Apart from their immunosuppressive actions, other clinical effects of these

[†] Supported by Ministry of Education Singapore ARC Grants T206B3217 (H.S.Y.) and MLC3/03 (J.L.). Financial support via Grants from the Singapore Biomedical Research Council (05/1/22/19/405) and ATIP from the CNRS to the J.L. laboratory is also acknowledged.

[‡] Coordinates have been deposited as Protein Data Bank entry 2VN1.

* To whom correspondence should be addressed. J.L.: e-mail, julien@ntu.edu.sg; telephone, +65-63162859; fax, +65-67913856. H.S.Y.: e-mail, hsyoon@ntu.edu.sg; telephone, +65-63162846; fax, +65-67913856.

[§] Nanyang Technological University.

[||] CNRS UMR6098.

[1] Abbreviations: FKBP, FK506-binding protein; PPIase, peptidylprolyl cis−trans isomerase; FKBD, FK506 binding domain; TPR, tetratricopeptide repeat; rms, root-mean-square; PDB, Protein Data Bank; CsA, cyclosporin A; NMR, nuclear magnetic resonance; NOE, nuclear Overhauser effect.

10.1021/bi800004u CCC: $40.75
Published on Web 05/09/2008

Table 1: Data Collection Statistics for the PfFKBD−FK506 Complex

X-ray source	ID14EH1, ESRF
wavelength (Å)	0.933
space group	$P4_32_12$
unit cell dimensions (a, b, c; α, β, γ)	63.1 Å, 63.1 Å, 168.0 Å; 90°, 90°, 90°
no. of molecules per asymmetric unit	2
resolution (Å)	30.0−2.35 (2.43−2.35)[a]
completeness (%)	99.8 (100)[a]
no. of reflections	308482
no. of unique reflections	14883
average $I/\sigma(I)$	41.1 (8.5)[a]
R_{merge} (%)	9.7 (38.2)[a]

[a] Statistics of highest-resolution shell are given in parentheses.

Table 2: Refinement Statistics and Quality Indicators

no. of reflections (working set/test set)	14092/733
R factor (R_{work}/R_{free})	0.195/0.251
no. of atoms (protein/water/ligand)	1938/164/104
mean B factors (Å^2) (protein/water/ligand)	34.9/36.5/24.5
rmsd for bonds (Å)	0.005
rmsd for angles (deg)	1.25
Ramachandran plot[a]	
residues in the most favored regions (%)	92.3
residues in the additionally allowed regions (%)	7.7
residues in the generously allowed regions (%)	0
residues in the disallowed regions (%)	0

[a] As defined by PROCHECK (*42*).

drugs may involve alternative mechanisms, leading to the speculation that FK506 has potentially multiple targets in various tissues and organisms (*8*). Using a *P. falciparum* parasite culture, Bell and colleagues demonstrated that FK506 has antiparasitic activity (*9*). The search for the molecular target of FK506 in the parasite resulted in the identification and characterization of a single new member of the FKBP family of proteins that was christened PfFKBP35 (*10–12*). PfFKBP35 is a 35 kDa protein with an N-terminal FK506 binding domain, a tripartite tetratricopeptide repeats (TPR) domain, and a putative calmodulin-binding module at its C-terminus. PfFKBP35 belongs to the subfamily of large FKBP proteins that includes several human proteins such as FKBP38, FKBP51, and FKBP52. The PfFKBP35 protein exhibits PPIase activity and assists protein folding, suggesting that it also functions as a chaperone enzyme in the parasite (*10, 12*). Both the PPIase and chaperone activities can be inhibited by FK506 (*10, 12*) as well as by FK520 and several of their non-immunosuppressive analogues (*13*). Of great interest, several non-immunosuppressive analogues of FK520 inhibit *P. falciparum* growth, when present in the cell culture medium in the micromolar concentration range (*13*). Thus, PfFKBP35 is a possible target for antimalarial drug discovery. With the aim of assisting the design of FK506 analogues that would be both more specific toward the parasite enzyme and devoid of immunosuppressive activity, we determined the X-ray crystallographic structure of FKBD from PfFKBP35 (hereafter named PfFKBD) as a complex with FK506 to a resolution of 2.35 Å. We compare this structure with the previously reported solution structure of the free FKBD domain of PfFKBP35 determined by NMR (*14*). Several regions of the PfFKBD protein change conformations upon binding, including aromatic residues that make direct contact with the ligand, as shown by NMR experiments. In spite of an overall well-conserved ligand binding site compared to human FKBP12 described earlier, the PfFKBD structure reveals subtle differences in strands $\beta3$ and $\beta4$ and the $\beta3-\beta4$ loop and in the $\beta5-\beta6$ segment that lines the FK506 binding pocket. Of note, two of its residues are 4−5 Å from the nearest atom of the ligand, providing opportunities to alter the FK506 compound to increase its specificity for the *Plasmodium* parasite protein. Finally, using microarray analysis, we show that FK506 and CsA affect the transcription profile of the "early shizont" development in an analogous manner, leading to developmental arrest and parasite death.

MATERIALS AND METHODS

Protein Expression and Purification. PfFKBD was cloned with a hexahistidine tag at its C-terminal end, expressed, and purified as described previously (*15*). Briefly, the coding sequence of PfFKBD was amplified from the genomic DNA of *P. falciparum* strain 3D7 and cloned into pET29b. The plasmid was transformed into *Escherichia coli* BL21(DE3) cells which were grown at 37 °C in the presence of kanamycin, until OD_{600} reached 0.7. Protein expression was induced with 1 mM IPTG and was carried out at 25 °C for 3 h. The recombinant protein was purified by Ni-NTA metal affinity purification followed by gel filtration.

Crystallization and Data Collection. An automated initial crystallization screen was performed using a CyBio-crystal creator robot (Jena Biosciences) with the protein at a concentration of 15 mg/mL that had been previously mixed with the FK506 ligand to a final concentration of 1 mM. A volume of 200 nL of the mixture was added to an equal volume of the crystallization solution using the sitting drop vapor diffusion method. Crystals were obtained at 291 K with the "Grid Screen Sodium Malonate" (Hampton Research) using the precipitating solution (3.4 M sodium malonate at pH 4). After optimization, larger crystals up to 0.2 mm × 0.2 mm × 0.1 mm in size were grown using 2.7 M sodium malonate at pH 5. Before data collection, crystals were transferred to a cryoprotecting solution containing 3.4 M sodium malonate at pH 5 and cooled to 100 K in a gaseous nitrogen stream using an Oxford cryosystem. Diffraction intensities were collected at the ESRF (Grenoble, France) to a resolution of 2.35 Å using one single crystal and were integrated with DENZO and merged and scaled using SCALEPACK (*16*).

Structure Solution, Refinement, and Model Analysis. The structure of the complex between the PfFKBD protein and FK506 was determined using the molecular replacement software MrBUMP (*17*) with the FKBD protein from yeast (PDB entry 1YAT) (*18*) as a search probe. The structure was refined using molecular dynamics and simulated annealing as implemented in CNS (*19*), with positional and individual temperature factor refinement. Throughout the whole refinement procedure, noncrystallographic restraints were applied between the two independent molecules of the asymmetric unit. The computer graphics software O was used for model rebuilding between refinement cycles (*20*). Analysis of the atomic model was carried out with the CCP4 suite of programs (*21*). The refined coordinates and structure factor amplitudes have been deposited in the PDB as entry 2VN1. A model of a ternary complex of PfFKBD, FK506, and

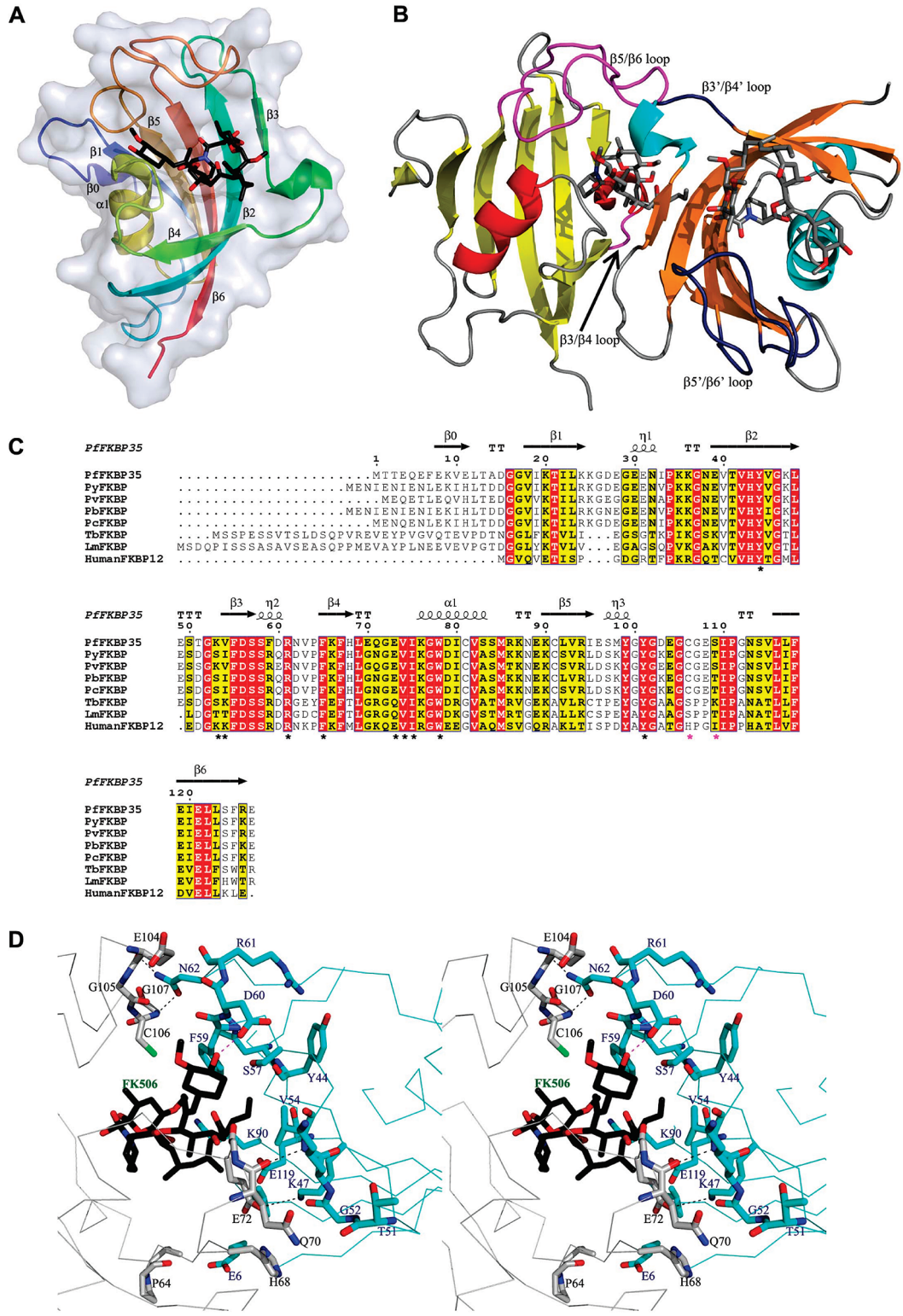

FIGURE 1: (A) Representation of the complex formed between the FK506 binding domain of PfFKBP35 and FK506 (represented as sticks with carbon atoms colored black and oxygen atoms red). The protein secondary structures elements are labeled and colored from blue at the N-terminus to red at the C-terminus. (B) Representation of the PfFKBD dimer present in the asymmetric unit. Helices are colored red and cyan and sheets yellow and orange. Bound FK506 molecules are shown as sticks. The $\beta3-\beta4$ and $\beta5-\beta6$ loops are colored purple (molecule A) and dark blue (molecule B, prime). (C) Sequence alignment of the FK506 binding domain from PfFKBP35 with FKBDs from other parasites: PyFKBP, *Plasmodium yoeli yoeli* FKBP (GenBank accession code XP_730233); PvFKBP, *P. vivax* FKBP (XP_001613999); PcFKBP, *Plasmodium berghei* FKBP (XP_672280), *Plasmodium chabaudi* FKBP (XP_736859); PbFKBP, TbFKBP, *T. brucei* FKBP (XP_828079); LmFKBP, *L. major* FKBP (XP_001682742). The secondary structure elements shown above the alignment are for the complex between PfFKBD and FK506. The black asterisks below the alignment indicate conserved residues within the FK506 binding site, while the purple asterisks indicate Cys106 and Ser109 of the $\beta6-\beta7$ loop (see the text). Strictly conserved residues are highlighted in red and partially conserved residues in yellow. (D) Stereoview of the intermolecular interface formed between the two independent PfFKBD molecules (colored gray and cyan) in the asymmetric unit. The FK506 molecule trapped in the interface is colored black. Hydrogen bonds are shown as dashed lines.

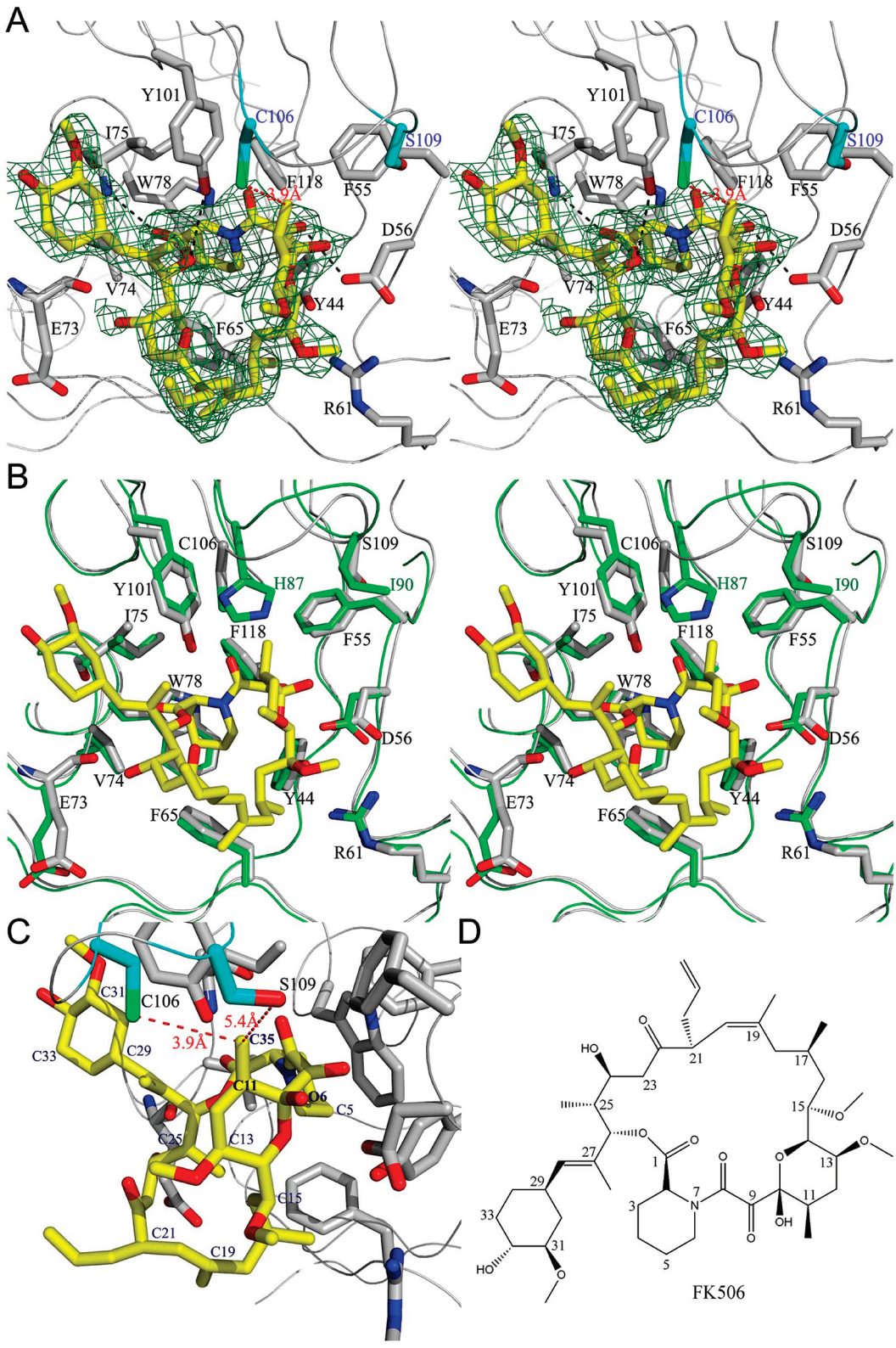

FIGURE 2: FK506 binding site of PfFKBD. (A) Stereoview of the simulated annealing difference Fourier map with $|F_{obs}| - |F_{calc}|$ coefficients and phases calculated from the protein model with atoms from the ligand omitted and contoured at a level of 3σ. The bound FK506 molecule is displayed as yellow sticks. Residues from PfFKBD interacting with FK506 are colored gray and labeled. Hydrogen bonds are represented by black dashed lines. Residues Cys-106 and Ser-109 are colored cyan (see the text). The shortest distance between the ligand and the PfFKBD protein is between Cys-106 and the methyl group C35 from FK506 and is 3.9 Å (shown as a red dashed line). (B) Stereoview of the superposition of the FK506-binding site of PfFKBD (gray) and human FKBP12 (green). Residues binding FK506 are labeled. Differences between the two binding pockets are at residues His-87 and Ile-90 of human FKBP12 which are substituted with Cys-106 and Ser-109, respectively, in the *P. falciparum* enzyme (see the text). (C) View from a different angle of the FK506 binding site of PfFKBD. Residues Cys-106 and Ser-109 are highlighted in cyan, and their distances from the nearest atoms of the FK506 ligand are indicated as red dashes. The atoms of FK506 are labeled with the positions of atoms C11, C35, and O6 highlighted in bold. (D) Chemical structure of FK506 (tacrolimus). Substitutions of the methyl group at position 11 of the macrocycle might render the compound more specific toward the *P. falciparum* enzyme (see the text).

Table 3: Interactions between FK506 and PfFKBD

Nonpolar Contacts[a]	
ligand region	PfFKBD residues
C1	V74, I75, Y101
C2−N7	Y44, F65, V74, W78, Y101
C8−C9	Y44, F55, D56, Y101, F118
C10−C14	Y44, D56, Y101, **C106**, I110
C15−C17	Y44, D56, R61, F65
C24−C26	F65, E73
C27−C34	I75, (**G100**), Y101

Hydrogen Bonds		
ligand	PfFKBD	donor−acceptor distance (Å)
C1 carbonyl	I75 N	3.14
C8 carbonyl	Y101 OH	2.75
C10 hydroxyl	D56 Oβ	2.69
C24 hydroxyl	E73 carbonyl	2.62
C9 carbonyl	Y44 CβH	3.72
C9 carbonyl	F55 CβH	3.24
C9 carbonyl	F118 CβH	3.58

[a] Nonpolar contacts are shown for distances of <4.0 Å. The two amino acid substitutions compared to human FKBP12 are shown in bold. The carbonyl oxygen of Gly-100 (which substitutes for Ala-81 in human FKBP12) is 4.53 Å from the C45 methyl group of FK506 and thus no longer in direct contact with the ligand, as was the case for the corresponding carbonyl oxygen of Ala-81 in human FKBP12 (distance of 3.44 Å).

calcineurin was obtained by superposition of PfFKBD as a rigid body onto the human FKB12 of the ternary complex (PDB entry 1TCO), using the CCP4 suite of programs.

NMR Sample Preparation. For NMR experiments, the uniformly ^{15}N-labeled or ^{15}N- and ^{13}C-labeled PfFKBD was prepared by growing the cells in the M9 medium supplied with 1 g/L $^{15}NH_4Cl$ or 1 g/L $^{15}NH_4Cl$ and 1g/L [^{13}C]glucose (*22*). The purified sample contained 20 mM $NaPO_4$ (pH 6.5), 50 mM NaCl, 1 mM DTT, and 0.01% NaN_3 in a 9:1 H_2O/D_2O mixture, with a final protein concentration of 0.5 mM. FK506 (Tacrolimus) was purchased from LC Laboratories (Woburn, MA). The 1:1 complex sample of PfFKBD and FK506 was prepared from PfFKBD by addition of FK506 and by monitoring two-dimensional (2D) ^{1}H−^{15}N HSQC spectra until the protein was saturated. Excess FK506 was removed by centrifugation. The final protein concentration in the complex is 0.5 mM.

NMR Backbone Assignment and NOESY Experiments. All backbone assignment and NOESY experiments (*23, 24*) for the ^{15}N- and ^{13}C-labeled or ^{15}N-labeled 1:1 PfFKBD−FK506 complex were carried out at 298 K on a Bruker Avance 700 MHz spectrometer equipped with a cryoprobe accessory. Backbone ^{1}H, ^{15}N, and ^{13}C resonances were assigned using data from 2D ^{1}H−^{15}N HSQC, three-dimensional (3D) HNCACB, and 3D CBCA(CO)NH spectra (*23*). 3D ^{15}N-edited and -filtered NOESY spectra were acquired with a mixing time of 100 ms. Spectra were processed using Topspin version 1.3 (Bruker) and analyzed with Felix (Accelrys).

Heteronuclear Single-Quantum Correlation (HSQC) NMR Spectroscopy and Chemical Shift Perturbation Analysis. Chemical shift perturbations to ^{15}N-labeled PfFKBD were monitored on a series of 2D ^{1}H−^{15}N HSQC spectra collected at 298 K with varying molar ratios between the uniformly ^{15}N-labeled protein and FK506 on the 700 MHz NMR spectrometer.

NMR Relaxation Measurements. ^{1}H−^{15}N heteronuclear nuclear Overhauser effect (NOE) measurements were carried out on the 700 MHz spectrometer as described previously (*25, 26*). The NOE values were measured using a 2 s interscan delay followed by either proton saturation for 3 s using a series of 120° ^{1}H pulses or an additional 3 s delay at 298 K for free PfFKBD and the 1:1 PfFKBD−FK506 complex. Data were processed by using NMRPipe (*27*) and NMRView (*28*).

Microarray Analysis. We analyzed the global transcription response of *P. falciparum* to the FK506 and cyclosporin inhibitors (purchased from Sigma). *P. falciparum* parasites were treated at the early schizont stage (~32 h post-invasion, hpi) with either 200 nM cyclosporin A (CsA) or 250 nM FK506 (corresponding to approximately 2 × IC_{90} concentrations for each inhibitor). Genome-wide gene expression profiling was conducted using a long oligonucleotide representing all 5363 *P. falciparum* genes (*29*), and the microarray hybridizations were carried out as previously described (*30*). For these experiments, early schizonts of *P. falciparum* (32 hpi) were treated with IC_{50} concentrations of either CsA or FK506 and mRNA abundance was measured in samples collected over a period of 8 h.

RESULTS AND DISCUSSION

Overall Structure. Details of the X-ray data collection statistics are given in Table 1. Refinement parameters defining the quality of the atomic model of PfFKBD are listed in Table 2. The refined crystallographic structure contains 123 amino acid residues for the two independent molecules present in the asymmetric unit. Missing amino acids are located at the N-terminal ends of each monomer which could not be traced presumably because of their high mobility in the crystal. The FK506 binding domain of PfFKBP35 features a half-β-barrel composed of a seven-stranded β-sheet and a short α-helix that sits on the β-sheet platform (Figure 1A). While PfFKBD shares 79% amino acid sequence identity with its homologue protein from *P. vivax* which is the other major etiologic agent of malaria in humans, it reveals more divergent relationships with homologous proteins from other parasites. Sequence alignments of PfFKBD with FKBD proteins from *Trypanosoma brucei* and *Leishmania major* reveal amino acid identity levels of 52 and 50%, respectively (Figure 1C). In particular, the residues that provide direct contact to FK506 are well conserved across all species, including human FKBP12, in spite of a low overall level of sequence identity of 42% (Figure 1C). The two PfFKBD monomers present in the asymmetric unit can be superposed with an average rms deviation of 0.37 Å for 122 α-carbon atoms. The two independent PfFKBD molecules are related by an improper noncrystallographic axis of rotation of 136° with a residual translation needed to bring them into coincidence. Their interface is formed by residues that emanate from the β3−β4 and β5−β6 loops with the formation of several hydrogen bonds that involve residues Gln-71, Glu-73, Glu-104, and Gly-107 of one monomer with Asn-62, Val-54, Lys-47, and Asn-62 of the other monomer. The accessible surface area buried in the interaction is 369 Å^2. Interestingly, this interface is partially mediated by an exposed region of the bound FK506 ligand, which is sandwiched between the two independent monomers and makes several, mostly hydrophobic, contacts with strands

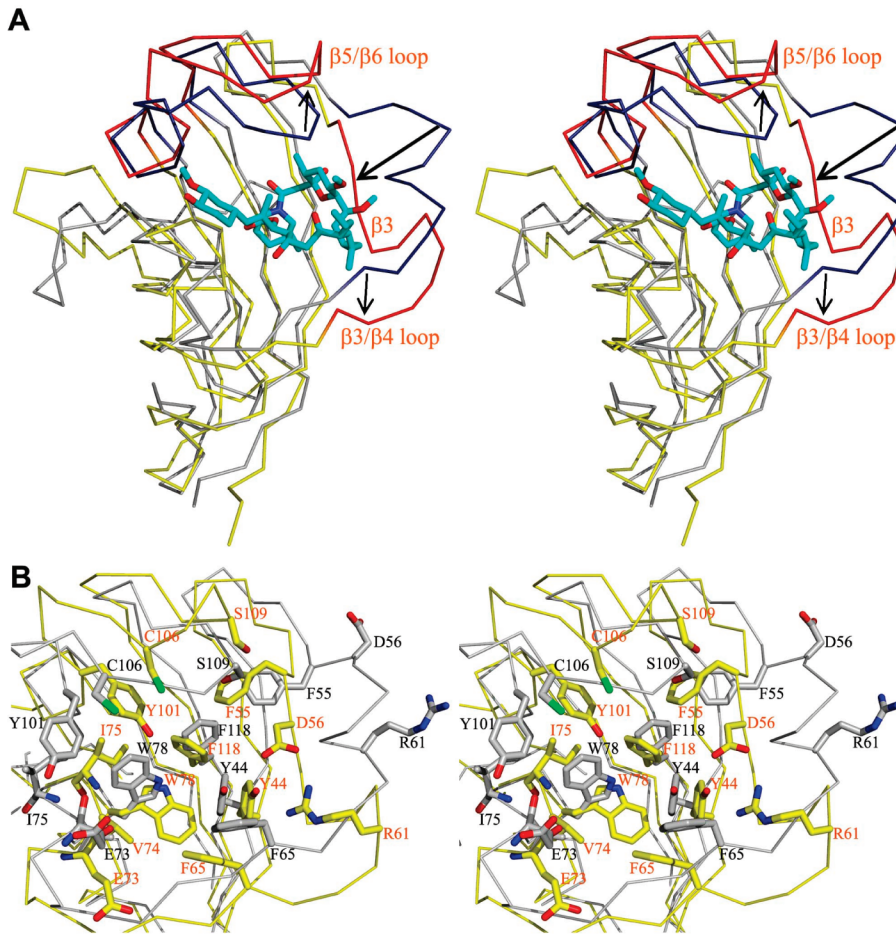

FIGURE 3: FK506-induced conformational changes within the PfFKBD protein. (A) Stereoview of the superposition of Cα traces from the solution structure of unliganded PfFKBD in gray with $\beta3-\beta4$ and $\beta5-\beta6$ loops colored dark blue (PDB entry 2OFN) and of FK506-bound PfFKBD colored yellow ($\beta3-\beta4$ and $\beta5-\beta6$ loops colored red). Regions undergoing large conformational changes are marked with arrows and labeled. Strand $\beta3$ is also labeled. (B) Close-up stereoview of the FK506-binding site. Residues are colored gray for apo-PfFKBD and yellow for the FK506-bound structure. The FK506 molecule was omitted for clarity.

$\beta2$, $\beta3$, and $\beta6$ of the other monomer (Figure 1B,D). One hydrogen bond is formed between the C32-hydroxyl moiety of FK506 and the oxygen amide of Asp-60 from the neighboring PfFKBD (Figure 1D). The second monomer roughly occupies the location of the calcineurin in the FKBP−FK506−calcineurin ternary complex. However, PfFKBD elutes as a monomer in solution as shown by gel filtration experiments (*15*). From a structure-based alignment (Figure 1C), we infer that residue Asp-56 of the parasite protein should play an essential role in its PPIase activity since mutation of the equivalent residue, Asp-37, to Val inactivates the human FKBP12 enzyme (*31*).

PfFKBD−FK506 Complex. Unambiguous residual difference electron density for one FK506 molecule per monomer was found in the ligand-binding pocket, a shallow cavity located between helix α1 and the β-sheet platform (Figure 2A). FK506 appears well-ordered with temperature factors similar to those of neighboring protein side chain atoms that make contact with the ligand (Table 2). The buried surface area of 854 Å^2 for the interaction is comparable to values found for FK506 in complex with the human and yeast FKBP12 proteins. The binding pocket is lined with conserved residues Tyr-44, Phe-65, Val-74, Ile-75, and Phe-118 (Figures 1C and 2). $\beta3-\beta4$, $\beta4-\alpha1$, and $\beta5-\beta6$ loops (encompassing residues 57−64, 69−75, and 96−115, respectively) flank the binding pocket. The strictly conserved Trp-78 that emanates from the α-helix serves as the platform for the pipecolinyl ring of FK506 (Figure 2B). Other residues which are <3.9 Å from FK506 include Phe-55, Asp-56, Arg-61, Glu-73, and Tyr-101 (Figure 2B and Table 3). The network of hydrogen bonds which were observed in the interaction between human FKBP12 and FK506 (*32, 33*) is also present in the complex between FK506 and PfFKBD (Table 3).

Conformational Changes of PfFKBD upon Ligand Binding. The solution structure of the PfFKBD apoenzyme was determined previously by NMR spectroscopy (PDB entry 2OFN) (*14*). A superposition of the two PfFKBD structures returns an overall rms deviation of 2.3 Å for 111 α-carbon atoms. Via restriction of the comparison to the protein core (residues 18−26, 38−53, 72−101, and 111−125), the value is reduced to 1.5 Å. The temperature factors for the FK506-bound enzyme as well as the values of the rms deviation per residue compared to the apoenzyme are shown in Figure 6B. Conformational changes between the apo and FK506-bound structures are observed in the loops that connect strand $\beta3$ to strand $\beta4$, strand $\beta4$ to helix α1, and strand $\beta5$ to strand $\beta6$ that acts as a "flap" closing up onto the ligand (Figures 3A and 6). A conspicuous difference between apo and ligand-bound PfFKBD is the change in the direction of the main chain that occurs at residue 55 with its ψ angle switching from 124° to −15° upon FK506 binding. As a result, the whole region encompassing residues 55−64 shifts toward

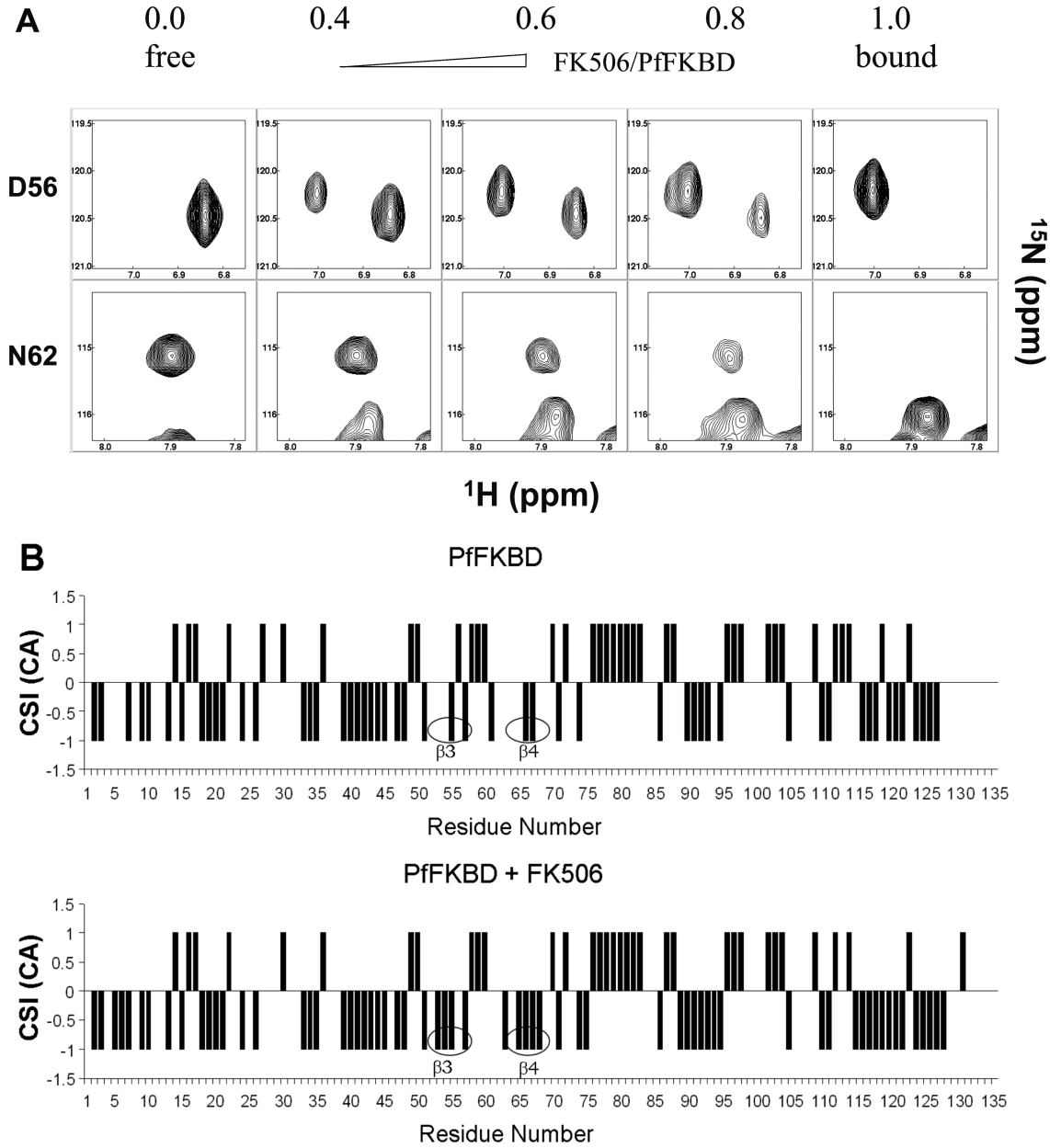

FIGURE 4: (A) Sections of the ^{1}H−^{15}N HSQC spectra recorded with ^{15}N-labeled PfFKBD in the presence of FK506. The chemical shifts of the indicated amino acids (Asp-56 in β3 and Asn-62 in the β3−β4 loop) were changed upon addition of increasing amounts of FK506. The numbers on the top indicate the molar ratios of FK506 to PfFKBD. Data were recorded at 298 K on a 700 MHz spectrometer. (B) CSI plots on ^{13}CA indicating secondary structure prediction. The observed chemical shifts were compared with random coil chemical shift standards, and a chemical shift index (−1, 0, 1) was assigned to each residue (*34*). The residues exhibiting the largest secondary structure changes are indicated with ovals. The changes with continuous negative values, which indicate a preference for β-stranded structure, were observed in portions of strands β3 (residues 53−57) and β4 (residues 65−68).

the ligand. The largest displacement is observed at residue 58 which moves by approximately 10 Å. This movement is accompanied by an extension of strand β3 and a shift of strand β4 toward the ligand by approximately 5 Å (Figure 3A). When FK506 binds, the β5−β6 flap also moves away from the ligand binding site as the position of Tyr-100 in the PfFKBD unliganded form would cause steric hindrance with FK506. The extension of β3 followed by movements of the β3−β4 and β4−α1 loops results in the shift of Ser-58 and repositions residues Phe-55, Asp-56, Arg-61, and Phe-65 for interaction with FK506. Accompanying movements of the side chains of residues Tyr-44, Glu-73, Ile-75, Trp-78, and Phe-118 are also observed in the crystal structure. As a caveat, we note that the β3−β4 region (but not the β5−β6 flap) is involved in crystal packing contacts with one symmetry-related molecule.

To rule out the effects that might be provoked by crystal packing contacts, we first performed 2D HSQC NMR titration experiments with ^{15}N-labeled PfFKBD by adding increasing amount of FK506. As shown in Figure 4A, chemical shift perturbations of the residues in the β3−β4 region were detected upon addition of FK506, suggesting that the change in the region is due to formation of the complex. We also compared NMR backbone chemical shift index (CSI) values between apo and ligand-bound PfFKBDs. CSI analyses (*34, 35*) on $^{13}C^{\alpha}$ (CA) and $^{13}C^{\beta}$ (CB) indicate that FK506-bound PfFKBD shares a similar secondary structure with apo-PfFKBD, except the portions of strands

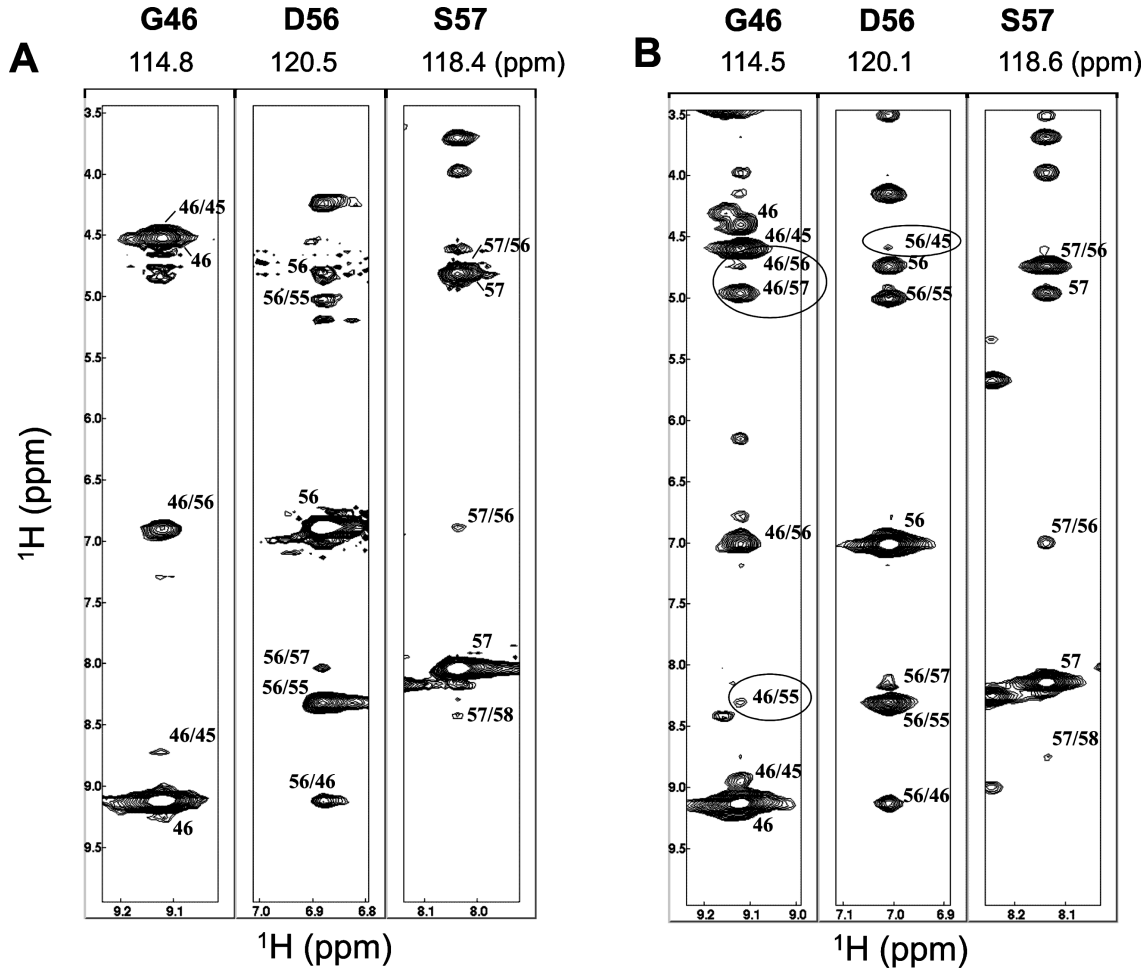

FIGURE 5: NOE strips showing cross-peaks for residues Gly-46, Asp-56, and Ser-57. Short- and long-range NOE cross-peaks are indicated in the slices of 3D ^{15}N-edited NOESY-HSQC spectra of free PfFKBD (A) and PfFKBD complexed with FK506 (B). The residues and the corresponding ^{15}N chemical shifts are indicated at the top of each slice, and the cross-peaks are identified by the residue number. Additional inter-residue NOEs detected in the complex are highlighted with ovals. The assignments of the NOEs were confirmed by comparing 3D ^{15}N-filtered NOESY-HSQC spectra.

β3 and β4 on CA (Figure 4B). CSI values of the complex predict that strands β3 and β4 are better defined upon FK506 binding and strand β3 in the complex is extended by including additional residues (53−57), as compared to the free PfFKBD NMR structure that shows strand β3 with fewer residues (53 and 54). The conformational change upon ligand binding is further confirmed by NOE connectivity. Additional inter-residue NOEs were detected upon complex formation; NOE cross-peaks between backbone amide protons of residues 46 and 55 appeared, and a strong NOE cross-peak between the α-proton of residue 57 and the amide proton of residue 46 was observed in the ligand-bound state (Figure 5). In addition, heteronuclear ^{1}H−^{15}N NOE measurements for the backbone amide of PfFKBD suggest that some of the residues located in the extended β3 (residues 55 and 57) and loops connecting strand β3 to strand β4 (residues 60−63) and strand β6 to strand β7 (residues 107−114) are rigidified in the presence of FK506 (Figure 6A), giving evidence to support the conformational changes in PfFKBD upon formation of the complex with FK506, under solution conditions.

Together, our NMR data are consistent with the structural difference observed between the free and ligand-bound PfFKBDs and also suggest that the solution structure of PfFKBD would resemble the crystal structure.

Comparison of FK506 Binding Sites of PfFKBD with Human FKBP12. The contacts established between FK506 and PfFKBD are listed in Table 3, allowing direct comparison with the human FKBP12 protein (PDB entry 1FKJ) (*32*). As seen in Figure 2B, residues that make direct contacts with the FK506 ligand are mostly conserved between the two proteins. Two major differences are found within the β5−β6 loop where His-87 and Ile-90 in human FKBP12 are replaced with Cys-106 and Ser-109, respectively, in PfFKBD. In the human FKBP12 protein, the side chains of these two residues form a complementary surface to the pyranose methyl group of FK506 and thus play a major role in ligand binding (*33*). However, in PfFKBD, the sulfhydryl and hydroxyl groups of the corresponding residues, Cys-106 and Ser-109, are 3.9 and 5.4 Å, respectively, from FK506 and are thus not in direct contact with the inhibitor (Figure 2C). Interestingly, sequence alignment of PfFKBP35 with FKBPs from other *Plasmodium* species revealed a strict conservation of Cys-106 across different *Plasmodium* species while residue 109 is either a serine or a threonine (Figure 1C).

A Model for the Complex between PfFKBD and Calcineurin. Previously, it was shown that recombinant PfFKBP35 reveals FK506-independent or -dependent inhibition on the phosphatase activity of calcineurin (*10, 12, 15*). To address

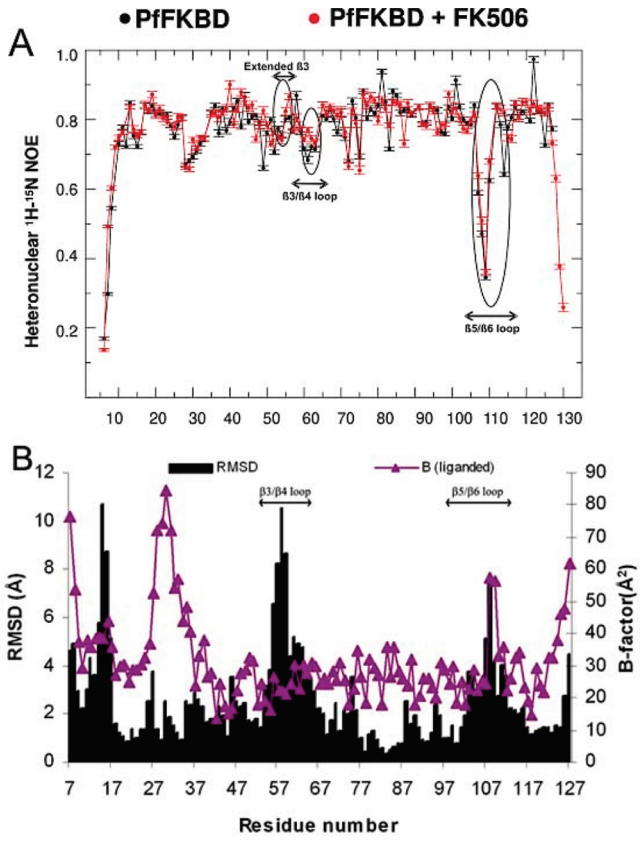

FIGURE 6: (A) Heteronuclear ^{1}H−^{15}N NOE for the backbone amides of PfFKBD. Backbone ^{1}H−^{15}N NOE values as a function of residue number for PfFKBD were measured. The NOE values for free PfFKBD and PfFKBD complexed with FK506 are colored black and red, respectively. The residues showing backbone dynamics changes are denoted with ovals. (B) Values of rmsd per residue between the free PfFKBD and PfFKBD complexed with FK506 (plotted as black bars). The temperature factors of the Cα atoms of PfFKBD complexed with FK506 are plotted as purple triangles. Regions showing the largest conformational changes are indicated.

the contradictory results and gain structural insights into the antimalarial effect of FK506, we used the X-ray structure of the ternary complex of human FKBP12 protein, FK506, and calcineurin (PDB entry 1TCO) (*36*) to model a putative complex involving the parasite PfFKBD enzyme (Figure 7). Sequence alignment shows that the regions of *P. falciparum* and bovine calcineurin involved in FKBP−FK506 binding are relatively conserved. Interactions between the PfFKBD−FK506 unit and calcineurin would involve atoms from the three partners with FK506 making contacts with Trp-352, Ser-353, Pro-355, Phe-356, and Glu-359 of the CnB-binding α-helix (BBH domain) of calcineurin (*36, 37*) and residues 51−56 (corresponding to residues 32−37 of human FKBP12) with its phosphatase domain. Our model suggests that the structural basis of binding between FK506 and PfFKBD is similar to that of FKBP12, where the composite surface of the PfFKBD−FK506 complex is critical for calcineurin inhibition and binding. However, several differences between the two ternary complexes are expected, since the $\beta3-\beta4$ loop of PfFKBD possesses an additional residue leading to a different conformation compared to the human FKBP12 protein and potentially different hydrophobic interactions with calcineurin. A major difference is observed in residues 106−109 of the $\beta5-\beta6$ loop (corresponding to residues 87−90 in the human FKBP12 protein) which interacts with the BBH domain. Their sequence is ^{106}CGES^{109} for PfFKBP35 and ^{87}HPGI^{90} for human FKBP12 (Figure 1B). Interestingly, as noted earlier, residues His-87 and Ile-90 which are important for calcineurin binding by the human FKBP12 protein (*36, 38, 39*) are substituted with Cys-106 and Ser-109, respectively, in PfFKBP35. It remains to be seen whether these substitutions would result in a loss of affinity for calcineurin as is the case for the human FKBP12 protein.

Opportunities for Targeting More Specifically the Plasmodium Enzyme. The availability of an experimental structure for the complex between FK506 and the FK506 binding domain of PfFKBP35 should stimulate the design of inhibitors that may have potential as novel antimalarial drugs using structure-based approaches. One could envision exploiting the subtle differences observed in the FK506 binding site between human FKBP12 and PfFKBP35 in the following way.

The C35 methyl group which is connected to C11 could facilitate the design of *Plasmodium*specific FK506 analogues by targeting the sulfhydryl group of Cys-106 (Figure 2C,D).

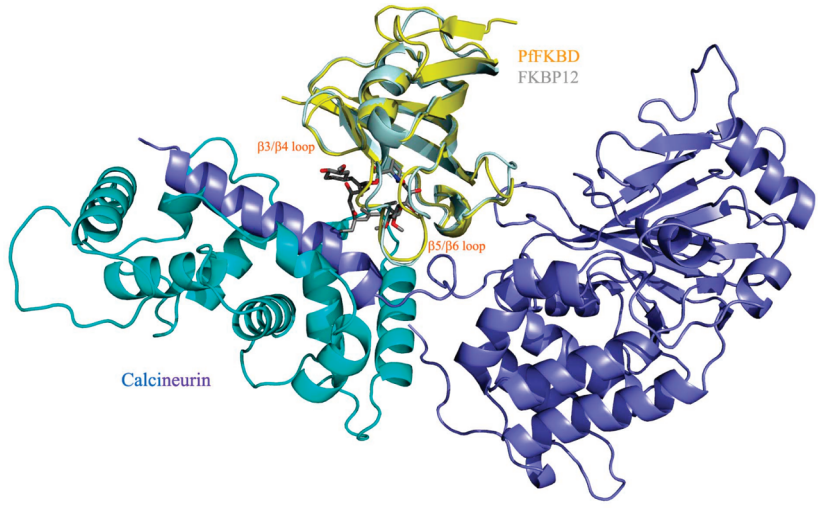

FIGURE 7: Putative ternary complex of FK506-bound PfFKBD and calcineurin. PfFKBD (yellow) was overlaid onto FKBP12 (pale cyan) of the FKBP12−FK506−calcineurin ternary complex to construct the ternary complex. FK506 is shown in sticks, and calcineurin is colored blue and cyan for subunits CnA and CnB, respectively.

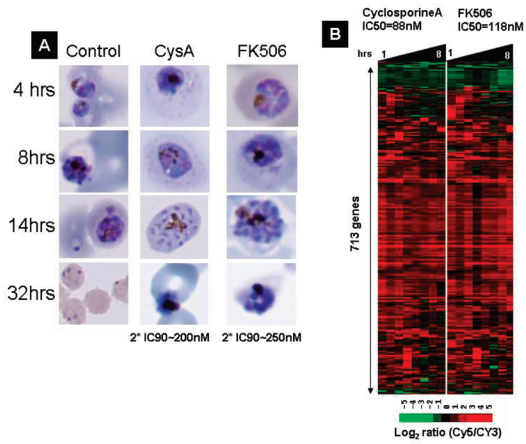

FIGURE 8: Effect of FK506 and cyclosporin A on *P. falciparum* development. (A) Parasite morphology was monitored by Giemsa stain microscopy 4, 8, 14, and 32 h after addition of inhibitor. During the first 14 h (schizont stage development), no significant morphological differences were observed between the treated and untreated parasites. During their subsequent development, the untreated controls progress to the next generation (formation of ring stages) while the treated cell remains arrested at the late schizont stage. The appearance of dense black shrunken (picnotic) cells 32 h post-treatment is consistent with parasite death. (B) Genome-wide gene expression profiling was conducted using a long oligonucleotide representing all 5363 *P. falciparum* genes. Expression profiles of 713 genes whose mRNA abundance was altered by >2-fold in at least one inhibitor treatment are indicated in the "heat map" generated by hierarchical clustering of the transcription profiles. The transcription profiles are represented as log2 ratios of relative mRNA abundance between treated and untreated *P. falciparum* parasites across the 8 h of the experimental time course. Good correlation in the global transcriptional response induced by both inhibitors points to a similar mode of action, inhibition of calcineurin-dependent signaling pathways.

Via insertion of an electrophilic group (e.g., a Br or Cl atom) at this position, a nucleophilic substitution reaction could lead to the formation of a covalently bound inhibitor solely for the parasite enzymes and not for the human FKBP12 enzyme which has a histidine residue at this position. Another option would be to create a Michael acceptor at the same position. Additional specificity for the parasite versus human FKBP12 enzyme could be conferred by elaborating on the O6 moiety of FK506 molecule to make use of the presence of Ser-109 in the same $\beta5-\beta6$ segment.

A Possible Mode of Action of FK506 in Inhibiting Growth of the P. falciparum Parasite. To improve our understanding of the biological function of PfFKBP35 and its potential as a target for antimalaria drug design, we studied the effect of FK506 on *P. falciparum* cells during the schizont stage development. In addition, we investigated the effect of cyclosporin A (CsA) which, like FK506, inhibits the calcineurin-dependent signaling pathway in other eukaryotic cells (*40, 41*). Interestingly, both FK506 and CsA did not appear to interfere with the schizont stage development but inhibited the egress of newly formed merozoites from the mature schizonts with 50% inhibitory concentrations (IC_{50}) of 118 and 88 nM, respectively (Figure 8A). This is in sharp contrast with two unrelated signaling pathway inhibitors Roscovitine (CDK-dependent kinase inhibitor) and ML-7 (myosin kinase inhibitor) which disturbed the parasite morphology already at early schizont stages (Z. Bozdech et al., manuscript in preparation). We analyzed the global transcription response of *P. falciparum* to these inhibitors. In agreement with the morphological studies (Figure 8A), we observed striking similarities between the effect of FK506 and CsA on the parasite cells (Figure 8B). Both inhibitors affected the transcription of 739 genes with 628 transcripts exhibiting a >2-fold increase in abundance. Although the majority of these genes are functionally uncharacterized (corresponding to 400 "hypothetical proteins"), this group also includes 56 genes from the variable surface antigen (VSA) gene families (27 *var.* and 29 *rifin*), 33 genes of ribosomal subunits, 18 genes from the apicoplast genome, seven protein kinases, and six enzymes involved in protein ubiquitination pathways. These data indicate that both FK506 and CsA affect the transcriptional profile of the early schizont development which underlines the eventual developmental arrest and subsequent parasite death. The specificity of the FK506/CsA-induced transcriptional response is further supported by the fact that two unrelated inhibitors of cell signaling pathways, ML-7 and Roscovitine, affected expression of distinct groups of genes with minimal overlaps (data not shown). Taken together our data suggest that PfFKBP35 appears to be essential for the progression of the *P. falciparum* life cycle. We speculate that the mode of FK506 and its antimalarial effect may be mediated through targeting PfFKBP35 and subsequent inhibition of the parasite calcineurin.

In conclusion, the results presented in this work might contribute to our understanding of the molecular mechanism of PfFKBP35 and its role in the parasite life cycle. Specific inhibition of this function could lead to severe disruption of parasite development in the host and thus validates PfKBP35 as a suitable target for malaria intervention strategies. Further inhibitor development should benefit from the detailed analysis of the *Plasmodium* enzyme binding site provided here.

ACKNOWLEDGMENT

We thank the ESRF for beamtime allocation. We thank Drs. E. P. Mitchell and S. Monaco for expert help with data collection, Dr. Cong Bao Kang for his help with NMR experiments, Jeff Tai for his help in purifying PfFKBD, and Drs. Liu Chuan Fa and Angus Bell for helpful discussions.

REFERENCES

1. World Health Organisation (2005) *World Malaria Report*.
2. Hyde, J. E. (2002) Mechanisms of resistance of *Plasmodium falciparum* to antimalarial drugs. *Microbes Infect. 4*, 165–174.
3. Weisman, J. L., Liou, A. P., Shelat, A. A., Cohen, F. E., Guy, R. K., and DeRisi, J. L. (2006) Searching for new antimalarial therapeutics amongst known drugs. *Chem. Biol. Drug Des. 67*, 409–416.
4. Kissinger, C. R., Parge, H. E., Knighton, D. R., Lewis, C. T., Pelletier, L. A., Tempczyk, A., Kalish, V. J., Tucker, K. D., Showalter, R. E., Moomaw, E. W., Gastinel, L. N., Habuka, N., Chen, X., Maldonado, F., Barker, J. E., Bacquet, R., and Villafranca, J. E. (1995) Crystal structures of human calcineurin and the human FKBP12-FK506-calcineurin complex. *Nature 378*, 641–644.
5. Galat, A. (2003) Peptidylprolyl cis/trans isomerases (immunophilins): Biological diversity−targets−functions. *Curr. Top. Med. Chem. 3*, 1315–1347.
6. Liu, J., Farmer, J. D., Jr., Lane, W. S., Friedman, J., Weissman, I., and Schreiber, S. L. (1991) Calcineurin is a common target of cyclophilin-cyclosporin A and FKBP-FK506 complexes. *Cell 66*, 807–815.

7. Feske, S., Okamura, H., Hogan, P. G., and Rao, A. (2003) Ca^{2+}/calcineurin signalling in cells of the immune system. *Biochem. Biophys. Res. Commun. 311*, 1117–1132.
8. Blankenship, J. R., Steinbach, W. J., Perfect, J. R., and Heitman, J. (2003) Teaching old drugs new tricks: Reincarnating immunosuppressants as antifungal drugs. *Curr. Opin. Invest. Drugs 4*, 192–199.
9. Bell, A., Wernli, B., and Franklin, R. M. (1994) Roles of peptidyl-prolyl cis-trans isomerase and calcineurin in the mechanisms of antimalarial action of cyclosporin A, FK506, and rapamycin. *Biochem. Pharmacol. 48*, 495–503.
10. Monaghan, P., and Bell, A. (2005) A *Plasmodium falciparum* FK506-binding protein (FKBP) with peptidyl-prolyl cis-trans isomerase and chaperone activities. *Mol. Biochem. Parasitol. 139*, 185–195.
11. Braun, P. D., Barglow, K. T., Lin, Y. M., Akompong, T., Briesewitz, R., Ray, G. T., Haldar, K., and Wandless, T. J. (2003) A bifunctional molecule that displays context-dependent cellular activity. *J. Am. Chem. Soc. 125*, 7575–7580.
12. Kumar, R., Adams, B., Musiyenko, A., Shulyayeva, O., and Barik, S. (2005) The FK506-binding protein of the malaria parasite, *Plasmodium falciparum*, is a FK506-sensitive chaperone with FK506-independent calcineurin-inhibitory activity. *Mol. Biochem. Parasitol. 141*, 163–173.
13. Monaghan, P., Fardis, M., Revill, W. P., and Bell, A. (2005) Antimalarial effects of macrolactones related to FK520 (ascomycin) are independent of the immunosuppressive properties of the compounds. *J. Infect. Dis. 191*, 1342–1349.
14. Kang, C. B., Ye, H., Yoon, H. R., and Yoon, H. S. (2007) Solution structure of FK506 binding domain (FKBD) of Plasmodium falciparum FK506 binding protein 35 (PfFKBP35). *Proteins 70*, 300–302.
15. Yoon, H. R., Kang, C. B., Chia, J., Tang, K., and Yoon, H. S. (2007) Expression, purification, and molecular characterization of *Plasmodium falciparum* FK506-binding protein 35 (PfFKBP35). *Protein Expression Purif. 53*, 179–185.
16. Otwinowski, Z., and Minor, W. (1997) Processing of X-ray Diffraction Data Collected in Oscillation Mode. *Methods Enzymol. 276*, 307–326.
17. Keegan, R. M., and Winn, M. D. (2007) Automated search-model discovery and preparation for structure solution by molecular replacement. *Acta Crystallogr. D63*, 447–457.
18. Rotonda, J., Burbaum, J. J., Chan, H. K., Marcy, A. I., and Becker, J. W. (1993) Improved calcineurin inhibition by yeast FKBP12-drug complexes. Crystallographic and functional analysis. *J. Biol. Chem. 268*, 7607–7609.
19. Brunger, A. T., Adams, P. D., Clore, G. M., DeLano, W. L., Gros, P., Grosse-Kunstleve, R. W., Jiang, J. S., Kuszewski, J., Nilges, M., Pannu, N. S., Read, R. J., Rice, L. M., Simonson, T., and Warren, G. L. (1998) Crystallography & NMR system: A new software suite for macromolecular structure determination. *Acta Crystallogr. D54* (Part 5), 905–921.
20. Martyn, D. C., Jones, D. C., Fairlamb, A. H., and Clardy, J. (2007) High-throughput screening affords novel and selective trypanothione reductase inhibitors with anti-trypanosomal activity. *Bioorg. Med. Chem. Lett. 17*, 1280–1283.
21. Collaborative Computational Project Number 4 (1994) The CCP4 suite: Programs for protein crystallography. *Acta Crystallogr. D50*, 760–763.
22. Kang, C. B., Feng, L., Chia, J., and Yoon, H. S. (2005) Molecular characterization of FK-506 binding protein 38 and its potential regulatory role on the anti-apoptotic protein Bcl-2. *Biochem. Biophys. Res. Commun. 337*, 30–38.
23. Sattler, M., Schleucher, J., and Griesinger, C. (1999) Heteronuclear multidimensional NMR experiments for the structure determination of proteins in solution employing pulsed field gradients. *Prog. NMR Spectrosc. 34*, 93–158.
24. Simon, B., and Sattler, M. (2004) Speeding up biomolecular NMR spectroscopy. *Angew. Chem., Int. Ed. 43*, 782–786.
25. Farrow, N. A., Muhandiram, R., Singer, A. U., Pascal, S. M., Kay, C. M., Gish, G., Shoelson, S. E., Pawson, T., Forman-Kay, J. D., and Kay, L. E. (1994) Backbone dynamics of a free and phosphopeptide-complexed Src homology 2 domain studied by ^{15}N NMR relaxation. *Biochemistry 33*, 5984–6003.
26. Vojnic, E., Simon, B., Strahl, B. D., Sattler, M., and Cramer, P. (2006) Structure and carboxyl-terminal domain (CTD) binding of the Set2 SRI domain that couples histone H3 Lys36 methylation to transcription. *J. Biol. Chem. 281*, 13–15.
27. Delaglio, F., Grzesiek, S., Vuister, G. W., Zhu, G., Pfeifer, J., and Bax, A. (1995) NMRPipe: A multidimensional spectral processing system based on UNIX pipes. *J. Biomol. NMR 6*, 277–293.
28. Johnson, B. A., and Blevins, R. A. (1994) NMR View: A computer program for the visualization and analysis fo NMR data. *J. Biomol. NMR 4*, 603–614.
29. Hu, G., Llinas, M., Li, J., Preiser, P. R., and Bozdech, Z. (2007) Selection of long oligonucleotides for gene expression microarrays using weighted rank-sum strategy. *BMC Bioinf. 8*, 350.
30. Bozdech, Z., Zhu, J., Joachimiak, M. P., Cohen, F. E., Pulliam, B., and DeRisi, J. L. (2003) Expression profiling of the schizont and trophozoite stages of *Plasmodium falciparum* with a long-oligonucleotide microarray. *Genome Biol. 4*, R9.
31. Fischer, S., Michnick, S., and Karplus, M. (1993) A mechanism for rotamase catalysis by the FK506 binding protein (FKBP). *Biochemistry 32*, 13830–13837.
32. Wilson, K. P., Yamashita, M. M., Sintchak, M. D., Rotstein, S. H., Murcko, M. A., Boger, J., Thomson, J. A., Fitzgibbon, M. J., Black, J. R., and Navia, M. A. (1995) Comparative X-ray structures of the major binding protein for the immunosuppressant FK506 (tacrolimus) in unliganded form and in complex with FK506 and rapamycin. *Acta Crystallogr. D51*, 511–521.
33. Van Duyne, G. D., Standaert, R. F., Karplus, P. A., Schreiber, S. L., and Clardy, J. (1991) Atomic structure of FKBP-FK506, an immunophilin-immunosuppressant complex. *Science 252*, 839–842.
34. Wishart, D. S., and Sykes, B. D. (1994) The ^{13}C chemical-shift index: A simple method for the identification of protein secondary structure using ^{13}C chemical-shift data. *J. Biomol. NMR 4*, 171–180.
35. Wang, Y., and Wishart, D. S. (2005) A simple method to adjust inconsistently referenced ^{13}C and ^{15}N chemical shift assignments of proteins. *J. Biomol. NMR 31*, 143–148.
36. Griffith, J. P., Kim, J. L., Kim, E. E., Sintchak, M. D., Thomson, J. A., Fitzgibbon, M. J., Fleming, M. A., Caron, P. R., Hsiao, K., and Navia, M. A. (1995) X-ray structure of calcineurin inhibited by the immunophilin-immunosuppressant FKBP12-FK506 complex. *Cell 82*, 507–522.
37. Ke, H., and Huai, Q. (2003) Structures of calcineurin and its complexes with immunophilins-immunosuppressants. *Biochem. Biophys. Res. Commun. 311*, 1095–1102.
38. Futer, O., DeCenzo, M. T., Aldape, R. A., and Livingston, D. J. (1995) FK506 binding protein mutational analysis. Defining the surface residue contributions to stability of the calcineurin co-complex. *J. Biol. Chem. 270*, 18935–18940.
39. Aldape, R. A., Futer, O., DeCenzo, M. T., Jarrett, B. P., Murcko, M. A., and Livingston, D. J. (1992) Charged surface residues of FKBP12 participate in formation of the FKBP12-FK506-calcineurin complex. *J. Biol. Chem. 267*, 16029–16032.
40. Liu, J. Farmer, J. D., Jr., Lane, W. S., Friedman, J., Weissman, I., and Schreiber, S. L. (1991) Calcineurin is a common target of cyclophilin-cyclosporin A and FKBP-FK506 complexes. *Cell 66*, 807–815.
41. Huai, Q., Kim, H. Y., Liu, Y., Zhao, Y., Mondragon, A., Liu, J. O., and Ke, H. (2002) Crystal structure of calcineurin-cyclophilin-cyclosporin shows common but distinct recognition of immunophilin-drug complexes. *Proc. Natl. Acad. Sci. U.S.A. 99*, 12037–12042.
42. Laskowski, R. A., MacArthur, M. W., Moss, D. S., and Thornton, J. M. (1993) PROCHECK: A program to check the stereochemical quality of protein structures. *J. Appl. Crystallogr. 26*, 283–291.

BI800004U